Advanced Ceramics Progress

Research Article

Preparation and Characterization of TiO$_2$ Nanoparticles Prepared by Sol-Gel Method

F. Mirjalili[a], S.A. Manafi[*b], I. Farahbakhsh[c]

[a]Department of Materials Engineering, Maybod Branch, Islamic Azad University, Maybod, Iran.
[b]Department of Engineering, Shahrood Branch, Islamic Azad University, Shahrood, Iran.
[c]Department of Engineering, Quchan Branch, Islamic Azad University, Quchan, Iran.

PAPER INFO

ABSTRACT

In this study, TiO$_2$ nanoparticles have been synthesized by sol-gel method in which aqueous solutions of titanium isopropoxide and ethanol were used to prepare the titania sol. CTAB and Span 20 were used as the surfactant stabilizing agent. Then, the effects of the different parameters such as pHs, stirring times, surfactants and temperatures on TiO$_2$ nanoparticles were studied. The X-ray diffraction (XRD), Fourier transforms infrared spectroscopy (FTIR), and transmission electron microscopy (TEM) analyses were used to characterize the samples. The observations revealed that the pH of 3.5 and 36 h stirring time could provide dispersion without agglomeration with rutile and anatase phases. However, at higher pH, the powder resulted in the formation of anatase phase. Using CTAB as a surfactant could modify the shape, size, and provide better distribution of TiO$_2$ nanoparticles compared with that of the Span 20 as a surfactant. Finally, the nanopowder was calcined at 450, 550 and 650 °C. It obviously showed that by increasing the temperature, the size of the nanoparticles increases to 30 nm which might be due to acceleration in the crystal growth of titanium dioxide at high calcination temperatures.

1. INTRODUCTION

Titania is a very well-known and well-researched material due to the constancy of its chemical structure, biocompatibility, physical, optical, and electrical properties. Its photocatalytic properties have been used in various environmental applications to remove contaminants from both water and air [1]. TiO$_2$ has three polymorphic forms of crystal structure namely brookite, anatase and rutile. Among other factors, this variation of applications of titanium dioxide is possible because of the properties like high stability, low cost, and non-toxicity [2].

Titania is usually utilized in the form of nanoparticles in suspension for the high catalytic surface area and activity [3]. However, TiO$_2$ nanoparticles in suspension are difficult to handle and are eliminated after being used in water and wastewater treatment [4]. TiO$_2$ nanostructures show an outstanding physiochemical properties, significantly different from bulky structure, like large specific surface area, extremely small size of

particles, and quantum size effect [1,5]. Recently, there has been considerable interest in the synthesis of titanium dioxide nanoparticles.
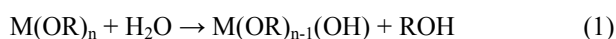
Over the past decade, the synthesis and functionalization of one-dimensional nanostructural materials have become one of the most highly energized research areas. Several methods have been used to synthesize nanosized TiO$_2$, such as sol-gel, hydrothermal, solvothermal, sonochemical, direct oxidation, electrodeposition, micelle and inverse micelle usage, emulsion or hydrolysis precipitation, chemical/physical vapor deposition, microemulsion processes, microwave approaches and ultrasonic [6-9]. These various studies consisted enormous number of varieties containing materials, experimental tools, instrumentations and experimental conditions. Consequently, researchers have to go through various preparation methods to get TiO$_2$ samples of certain preferred characteristics. [6-8,10]. Among the numerous preparation techniques, sol- gel is considered as one of the simple methods for synthesizing nanoparticles at ambient conditions. Besides, it does not require complicated set-up and the experimental conditions can be controlled easily [9,11,12].

*Corresponding Author's Email: ali_manafi2005@yahoo.com (S.A. Manafi)

In common sol-gel methods for preparing TiO$_2$ material, highly reactive alkoxide titanium precursors are violently hydrolyzed and further condensed to form the Ti–O–Ti network [5,8,9].

In sol-gel processes, TiO$_2$ is usually arranged by the reactions of hydrolysis and polycondensation of titanium alkoxide, (TiOR)n to form oxo-polymers, which are transformed into an oxide network [1,13]. These reactions can be schematically represented as follows:
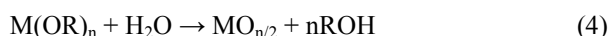
Hydrolysis:

$$M(OR)_n + H_2O \rightarrow M(OR)_{n-1}(OH) + ROH \quad (1)$$

Condensation and Dehydration:

$$M(OR)_n + M(OR)_{n-1} \rightarrow M_2O(OR)_{2n-2} + ROH \quad (2)$$

Dealcoholation:

$$2M(OR)_{n-1}(OH) \rightarrow M_2O(OR)_{2n-2} + H_2O \quad (3)$$

The overall reaction is

$$M(OR)_n + H_2O \rightarrow MO_{n/2} + nROH \quad (4)$$

where M= Si, Ti, Zr, etc. and R = alkyl group. The relative rates of hydrolysis and polycondensation strongly influenced the structure and properties of metal oxides. Factors that are crucial in the formation of metal oxides include reactivity of metal alkoxides, water to alkoxides ratio, pH of the reaction medium, nature of solvent and additives and reaction temperature. By varying these process parameters, materials with different surface chemistry and microstructure can be obtained [1,13,14].

Jimmy et al., investigated dispersion of nanoparticles using different methods which have become an essential and challenging issue [10]. In this regard, the tendency to coagulate can be defeated through the following methods: 1) Electrostatic revulsions between similarly charged particles, resulted from the creation of an electric double-layer, 2) Repulsive steric forces improving dispersion of solid particles by addition of organic mixtures, based on the interaction between the adsorption layers of admixture and 3) electrostatic mechanism generated by polyelectrolytes [10,11]. Behpour et al., [8] also described the effect of dispersants type and concentration on dispersion of two marketable and one synthesized titania nanopowders. They took the advantage of zeta-potential measurement and particle size distribution to characterize the nano titania suspensions.

In spite of a simplicity of sol-gel technique, some drawbacks limit its performance in nanoparticles synthesis such as spontaneous aggregation of primary particles, and small surface area of synthesized TiO$_2$ nanoparticles [13,15]. Therefore, one of the characteristic property of titanium dioxide is its ability to aggregate into large particles via chemical bounds [14,16]. Using the surfactants and different stirring time is the most effective method for preventing aggregation and powerful method for dispersing the particles in heterogeneous systems [1,17].

Most consideration in prior studies was concentrated on clarifying the response mechanisms and applying this simple methodology [15,18].

Previously, it was found that the anatase phase began to appear upon the calcination of the hydrolyzed species of titanium alkoxides at 450 $^\circ$C for 3 hours [19]. However, minor change in parameters such as pH, calcination temperature and stirring time considerably affect the TiO$_2$ characteristics. Consequently, different crystallinities and structures of TiO$_2$ can be achieved by controlling such parameters. Moreover, little work has been devoted to the fabrication of highly crystalline TiO$_2$ materials through a new synthesis method using surfactant molecules as a pore directing agent along with different stirring time-based sol–gel route. To this end, the novelty of this report is to obtain the optimum pH and stirring time and then modify the TiO$_2$ nanoparticles with different surfactants and different calcination times.

2. MATERIALS AND METHODS

TiO$_2$ nanopowders were prepared by solution sol-gel method using titanium isopropoxide (TTIP, 98%, Merck) with Ethanol (99.5%, Merck) and ammonia solution (25%, Merck) and hydrochloric acid (HCl, 25%, Merck) as the agent for pH adjustment as previously reported [15,20]. The suspensions of 2.5 ml titanium isopropoxide with 12.5 ml ethanol were vigorously stirred at 25 °C. After that, 2 ml distilled water was slowly added dropwise to the solution to form colloidal solution under vigorous stirrer and the resulting solution was stirred for different stirring times (24, 36, and 48 h) with adjusted different pH values of 1.8, 3.5, 7, 9 and then, the colloidal solution was dried in an oven at 110 °C for 8 h, and the obtained xerogel was calcinated at 450 °C for 2 h as shown in Fig. 1.

In the next part, for enhancing the properties, the effect of two surfactants (CTAB, Merck and Span 20, Merck) was investigated. The suspensions of ethanol with certain amount of surfactants (CTAB and Span 20) were vigorously stirred at 25 °C for 1 h. After that, the suspension of 2.5 ml titanium isopropoxide was added to the above solutions and then, 2 ml distilled water was slowly added dropwise to the solutions to form colloidal solution with adjusted pH and dried and the resulting solution was stirred for 36 h and calcinated at 450, 550 and 650 °C for 2 h.

Phase identification was performed by X-ray diffraction (XRD, PW1800, Philips) using nickel-filtered Cu-K$_\alpha$ radiation in the range of 2θ=5-80° with scanning speed of 5° min^{-1}. The relative accuracy was obtained in order of 10% at the 0.1% level. Fourier transform infrared

spectroscopy (FTIR, Perkin Elmer Spectrum 100) was conducted by the universal attenuated total reflection (UATR) method. Microstructures and morphology of

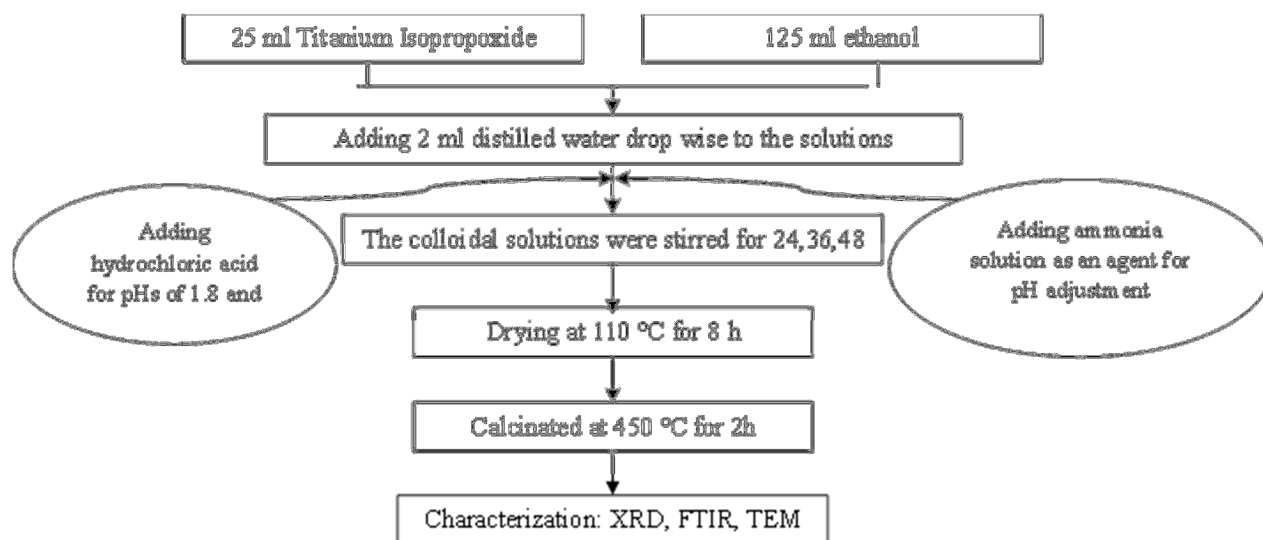powders were identified by transmission electron microscopy (Philip Netherlands).

Figure 1. Flow chart for preparation of TiO$_2$ nanopowders

3. RESULT AND DISCUSSION

The XRD patterns of the TiO$_2$ nanopowder with different pH (1.8, 3.5, 7, 9) are illustrated in Fig. 2. The sharp peaks emerged in the XRD pattern for pH of 1.8, 3.5 and 7 correspond to both anatase and rutile phases which is in agreement with Joint Committee on Powder Diffraction Standard (JCPDS) card PDF No. 76-1940 and 21-1272, respectively [21]. However, with increasing the pH from 7 to 9, only anatase phases remained. It can be seen that with increasing the pH from 1.8 to 9, the peak intensity of anatase phases at 19, 25, 37 and 47° was increased. Thus, the pH is expected to play a significant controlling role in the selective crystallization of anatase phase during sol-gel process [18,22]. This mechanism might be explained using the concept of partial charge model [1,19].
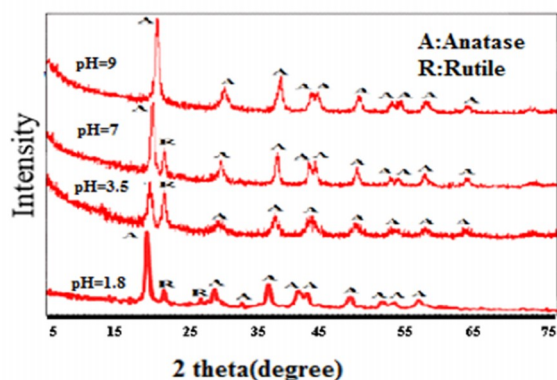
According to this model, hydrolysis of titanium cation was occurred at strong acidity condition. In this condition, a stable species of $[Ti(OH)(OH_2)_5]^{3+}$ would be formed, however; due to the positive charge of hydroxo group, these species were not able to condense. When acidity is not sufficiently low to stabilize this precursor, deprotonating would take place, forming new species of $[Ti(OH)_2(OH_2)_5]^2$.

However, these species also did not reduce probably because of spontaneous in intramolecular oxidation to $[TiO(OH_2)5]^{2+}$ [1,15,23]. Condensation to both anatase and rutile started when the solution movement was adequate to allow further deprotonating to $[TiO(OH)(OH_2)_4]^+$, which could undertake inter molecular deoxolation of $[TiO(OH)_3(OH_2)_3]^+$ depending on exact pH value. In lower pH region, deoxolation did not occur and oxidation led to linear growing along the equatorial plane of cations [1,19,24]. This led to rutile formation due to oxidation between resulting linear chains. Meanwhile, in higher pH values, when deoxolation occurred, condensation could progress along the apical direction and led to the twisted chain of anatase structure. [1,13,25]. The higher acidity provided rutile formation and lower acidity led to anatase formation. For these reasons, anatase and rutile phases were found in pH range of 1.8 to 7, but by increasing of pH from 7 to 9, only the anatase phase was created. The crystallite size of TiO$_2$ with various pH was also calculated using Scherrer equation (Table 1). The size of the crystalline was determined by the Scherrer method.

Figure 2. XRD patterns of nanocrystalline titania samples prepared by sol-gel method with various pH condition

The equation is as follows:

$$t = 0.89\lambda/\beta\cos\theta \qquad (5)$$

where, t is grain size, λ is the wavelength, β is peak width chosen at half height in radians and θ is the angle in degrees [10,15,26].

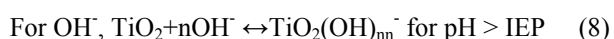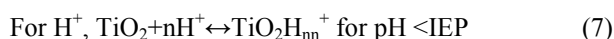$$\beta = (\beta_m^2 - \beta_s^2)^{1/2} \qquad (6)$$

where β_m, is the peak width at half-maximum of the sample and β_s is the peak width at half-maximum of the standard sample.

TABLE 1. The crystallite size of TiO_2 nanoparticles at different pH

τ (nm)	θ (°)	β (RAD)	pH
43	25.39	0.0032	1.8
36	25.33	0.0039	3.5
48	25.38	0.0029	7
53	25.41	0.0026	9

It is observed that, by increasing the pH from 3.5 to 9, the crystallite size of TiO_2 was increased.

According to several studies, the variety of TiO_2 surface charge was pH dependent. TiO_2 in sols possessed electrical charge because of the absorption of H^+ or OH^- in aqueous suspension. According to Saja et al. [1], the surface charges of TiO_2 could be determined by chemisorption of:

For H^+, $TiO_2 + nH^+ \leftrightarrow TiO_2H_{nn}^+$ for pH <IEP   (7)

For OH^-, $TiO_2 + nOH^- \leftrightarrow TiO_2(OH)_{nn}^-$ for pH > IEP   (8)

Moreover, the researchers concluded that the dispersed nanoparticles in a solvent tend to agglomerate and the electric potential is developed by an electric double layer called Zeta layer which is consisted of inner and outer layers. When all the particles have the same electrical charges they tend to separate and do not agglomerate and the repulsion of deposited particles is directly proportional to the zeta potential. When the zeta potential of solution is higher than +30 eV or lower than -30 eV, the solution is stable. Furthermore, the Zeta potential is reduced by increasing the pH to a point where the zeta potential reached zero, which is named as isoelectric point (IEP) [12,17,27].

For these reasons, the best dispersion condition of nanoparticles was seen at pH=3.5. The value of the zeta potential was decreased at higher potential. It causes a reduction of potential difference between the separated phases and its surrounding. Therefore, this was the main reason for the repulsion between the TiO_2 nanoparticles. At this condition, the Van der Waals forces were increased and resulted in agglomeration of TiO_2

nanoparticles. Taken together, the pH=3.5 is the best pH for preparing the TiO_2 nanoparticles.

The XRD patterns of TiO_2 nanoparticles with different stirring times are shown in Fig. 3. The XRD characteristic peaks revealed that, the main phases of all three samples were anatase and rutile phases. Furthermore, no significant difference was observed between them indicating that, the increase in stirring time does not affect the crystal structure of the final product. The crystalline size of nanopowders was calculated according to Scherer equation as shown in Table 2. It was observed that by the increase of stirring time to 36 h the crystallite size decreased. However, further increase of stirring time increased the crystallite size due to the agglomeration of nanoparticles. Takahashi and Yamaguchi [19] found that during stirring of a solution, the viscosity increased, therefore the particle size improved, however, due to the spinner revolution, the particle size decreased. So that with increasing the stirring time from 12 h to 36 h the crystallite size decreased. As it proceeded, after 36 h, more water evaporated from the sol, thus the supersaturated solution supplied the material necessary to bond colliding particles and form agglomerates. Moreover, this effect was probably due to Brownian forces that led to particle aggregation [18,28]. In addition, heat generated in the longer stirring time might be playing a factor in enhancing the movement of particles and particle aggregation [29]. Novakovic and Korthaus [19] have reported that drying of the sol invariably leads to agglomeration because the residual salts present in the sol form solid bridges between particles as the water evaporates.

TABLE 2. The crystallite size of TiO_2 nanoparticles prepared at different stirring times

τ (nm)	θ (°)	(RAD)β	hour (h)
49	25.40/2	0.1680	12
22	25.38/2	0.1200	36
38	25.39/2	0.2160	48

So that, with increasing the stirring time to 48 h, the crystallite sizes were increased. It is well understood that the 36 h stirring time is the optimum time for further surfactant treatment.

The XRD patterns of TiO_2-CTAB and TiO_2-Span 20 are shown in Fig. 4. The XRD characteristic peaks revealed that the main phase of all two samples was only anatase and there was not the rutile. Therefore, rapid crystallization of titania particles by adsorption on the surface of the titanium particles was achieved and only anatase phase was appeared.

The crystallite size of nanopowders was calculated   according to Scherer equation as shown in Table 3.
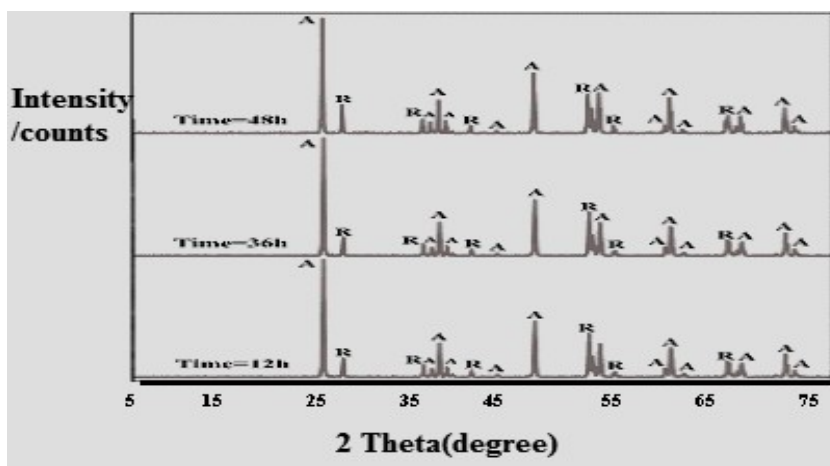

Figure 3. XRD patterns of nanocrystalline titania samples prepared by sol-gel method with various stirring time condition
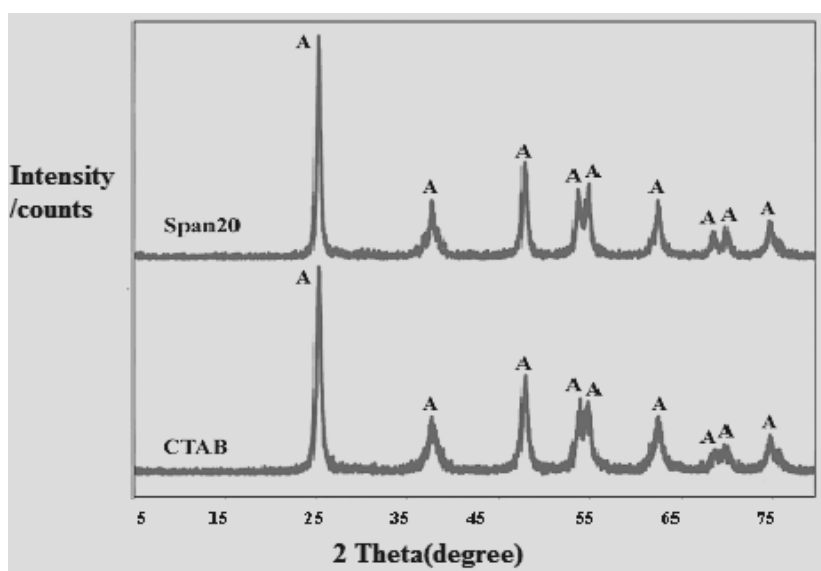

Figure 4. XRD patterns of nanocrystalline titania samples prepared by sol-gel method with various surfactants

It was observed that by increasing of CTAB as a surfactant, the crystallite size decreased. However, Span 20 as a surfactant did not play any significant role in dispersion of nanoparticles. In the case of cationic surfactant CTAB, low agglomeration, high dispersive and uniform crystallite size were obtained because of the electrostatic interaction between CTA^+ cations and $Ti\,(OH)_6^{2-}$ anions, and the cation CTA^+ condensed into aggregates in which counter ions $Ti\,(OH)_6^{2-}$ were related to the interfaces between the head group to form $CTA^+ - Ti\,(OH)_6^{2-}$ pair [30].

This might indicate a better dispersion, less agglomeration of nanoparticles with CTAB as well as more powder crystallization. Therefore, it was inferred that the best surfactant for TiO_2 nanoparticle is CTAB. The XRD patterns of TiO_2 nanoparticles with CTAB as

a surfactant at different temperatures are shown in Fig. 5.

TABLE 3. The crystallite size of TiO_2 nanoparticles with different surfactants

τ (nm)	θ (°)	β (RAD)	surfactant
16	25.3353/2	0.0089	CTAB
29	25.3259/2	0.0049	Span 20

The XRD patterns revealed that, the phase of all two samples at two temperatures was only anatase. Furthermore, no significant difference was observed between them indicating that the increase in temperature did not affect the phase structure of the final product.

However, TiO_2 nanopowder at 650 °C revealed a little bigger particle size and better powder crystallization.

The crystallite size of TiO_2 nanopowder at different temperature according to Scherer equation is shown in Table 4.

TABLE 4. The crystallite size of TiO_2 nanopowder at various temperatures

τ (nm)	θ (°)	β (RAD)	Temperature (°C)
34	25.4625/2	0.0043	550
37	25.3746/2	0.0037	650

By comparing the crystallite size of TiO_2 nanopowder, it is concluded that with increasing the temperature, the crystallite size was a little increased which might be, because of the acceleration of the crystal growth of titanium dioxide at high calcination temperature [23,30]. The FTIR spectra of calcined TiO_2 revealing the absorption band at 400-4000 cm^{-1} are shown Fig. 6. The TiO_2 powder showed absorbance peak in the range of 3500-3900 cm^{-1} related to vibration characteristics of O-H bond revealing the presence of water [14,25,31]. In addition, the peaks in the range of 2300-2400 cm^{-1} correspond to C-O bond revealing the presence of CO_2 from air, while the peak at 1700 cm^{-1} was due to the O-H bond revealing the presence of water [26]. Moreover, the bonds in the range of 800-1200 cm^{-1} belong to the Ti-O-Ti and Ti-O-O bonds [27,32].
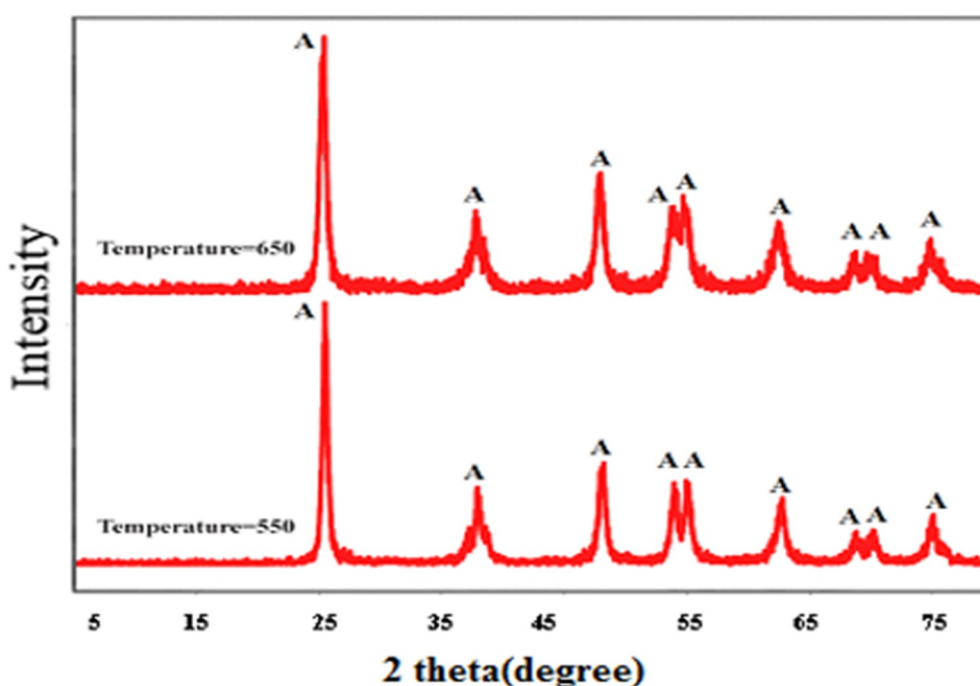

Figure 5. XRD patterns of nanocrystalline titania samples prepared by sol-gel method at various temperatures

The results showed that the obtained material after calcining is mostly the crystalline TiO_2.

The FTIR spectra of TiO_2 nanoparticles with different stirring times are also illustrated in Fig. 7. The vibration peaks in the rang of 800-1200 cm^{-1} are ascribed to Ti-O-Ti and Ti-O-O bonds [27, 33]. The peaks confirmed the formation of TiO_2 phase. The absorption band in the range of 3500-3900 cm^{-1} and 1700 cm^{-1} are related to vibration characteristics of O-H bond revealing the presence of water [29,34]. Moreover, with increasing the stirring time from 12 to 48 h the intensity of O-H bond was decreased revealing the water evaporation and loss of water of TiO_2 nanoparticles.

Fig. 8 shows the FTIR spectra of the TiO_2 nanoparticle with different surfactants. The vibration peaks in the range of 800-1200 cm^{-1} are ascribed to Ti-O-Ti and Ti-O-O bonds [28,35]. This confirmed the formation of TiO_2 phase which is in agreement with XRD result. The absorption bands in the range of 1380 and 1600 cm^{-1} was ascribed to the C-C characteristic peak related to hydrocarbon phase from surfactants [30,36]. The peaks confirmed the presence of CTAB and Span 20 as surfactants.

The FTIR spectra of TiO_2 calcined at different temperatures are also shown in Fig. 9. As mentioned before, the absorption band at the 800-1200 cm^{-1} was ascribed to Ti-O-Ti and Ti-O-O bonds which were confirmed the formation of TiO_2 phase. The vibration peaks in the range of 3500-3900 cm^{-1} and 1700 cm^{-1} are related to vibration characteristics of O-H bond revealing the presence of water [39]. According to Fig.

8, no significant difference was occurred between the spectra after increasing the temperature. However, after increasing the temperature all the peaks related to O-H

bond shifted to the lower absorbance which might be attributed to the evaporation and loss of water [10].
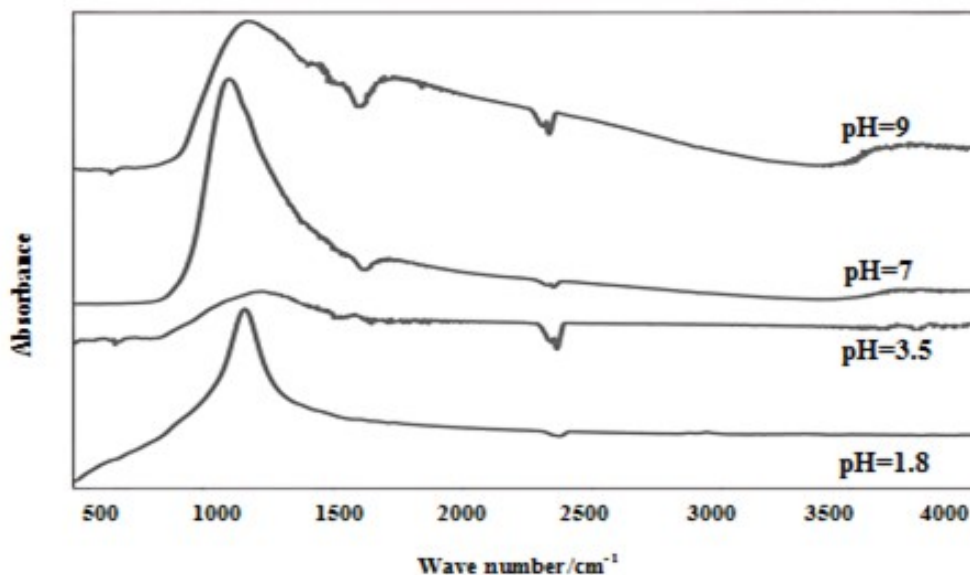

Figure 6. FTIR curves of nanocrystalline titania samples prepared by sol-gel method with various pH
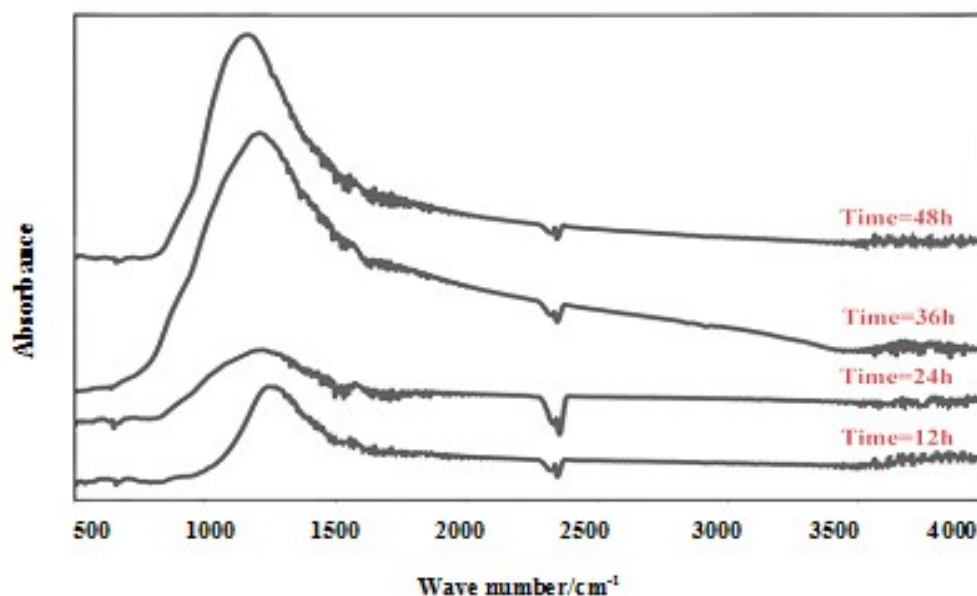

Figure 7. FTIR spectra of nanocrystalline titania samples prepared by sol-gel method with various stirring times

The morphology of calcined TiO$_2$ with the different condition was evaluated by TEM images as shown in Fig. 10. The TEM image of TiO$_2$ was used to investigate the particle size and morphology of TiO$_2$ nanopowders. As for the sample with pH=3.5. the particle size was in the range of 30-35 nm with spherical shape and they had better dispersion and less agglomeration than particles at pH=1.8.

As depicted in Fig. 10(a), TiO$_2$ nanopowder at pH=1.8 revealed the particle size around 38 nm with asymmetrical shape and some agglomeration.
The TEM micrograph of nano TiO$_2$ particles after 36 stirring times is also shown in Fig. 10(c). As it can be seen, the particle size was in the range of 20-25 nm with spherical shape and good dispersion and less agglomeration.

The TEM micrograph of TiO$_2$ capped with CTAB indicated that by adding surfactant, the dispersion of particles increased. Furthermore, the addition of surfactant improved the dispersion and formed nanoparticles with the sizes in the range of 16-20 nm with spherical shape (Fig. 10(d)). The CTAB surfactant was a cationic serviceable group which could accelerate the adsorption of Ti ions. Moreover, some negatively-charged groups were able to induce repulsive force for adsorption of Titanium (Ti^{4+}) ion and subsequent complexion with them. The TEM micrograph of TiO$_2$ at 650 °C is also shown in Fig. 10(f).
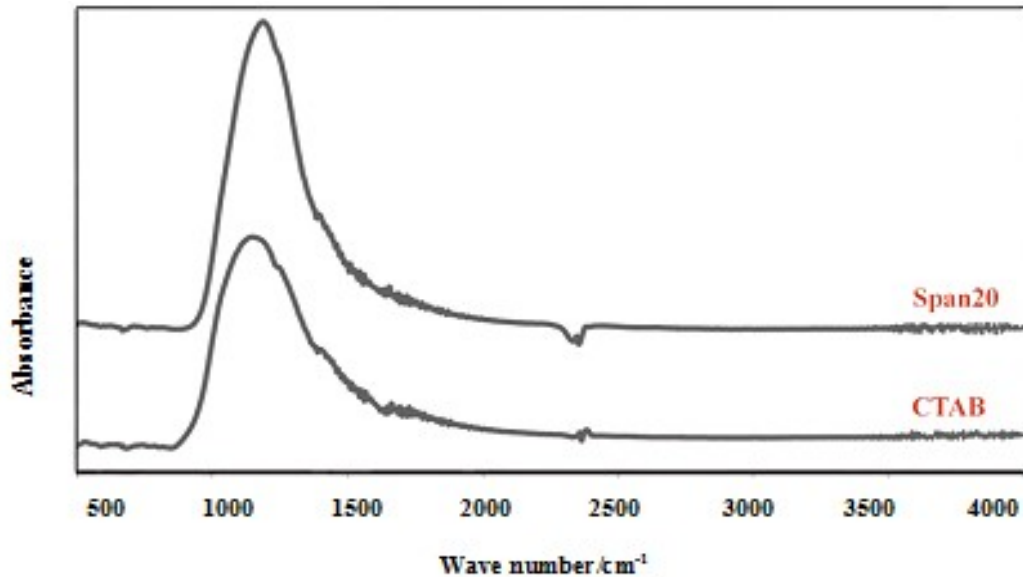

Figure 8. FTIR curves of nanocrystalline titania samples prepared by sol-gel method with various surfactants

It showed that by increasing the temperature, the size of particles increased to 30 -33 nm with spherical shape and good dispersion without any agglomeration which might be due to acceleration of the crystal growth of titanium dioxide at high calcination temperature [33,39].
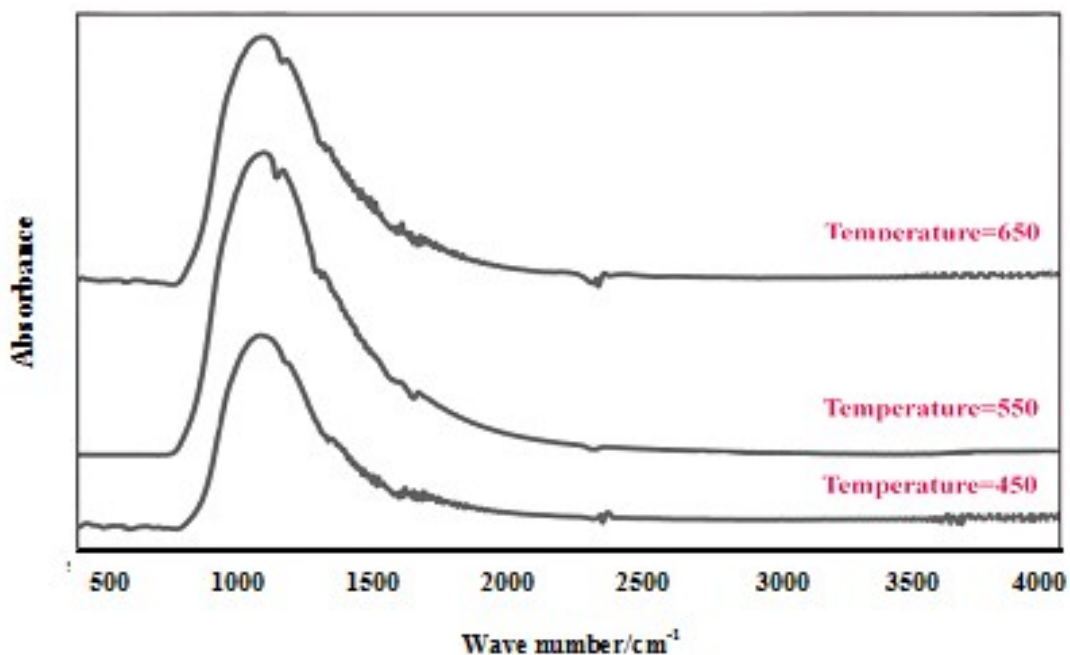

Figure 9. FTIR curves of nanocrystalline titania samples prepared by sol-gel method at various temperatures
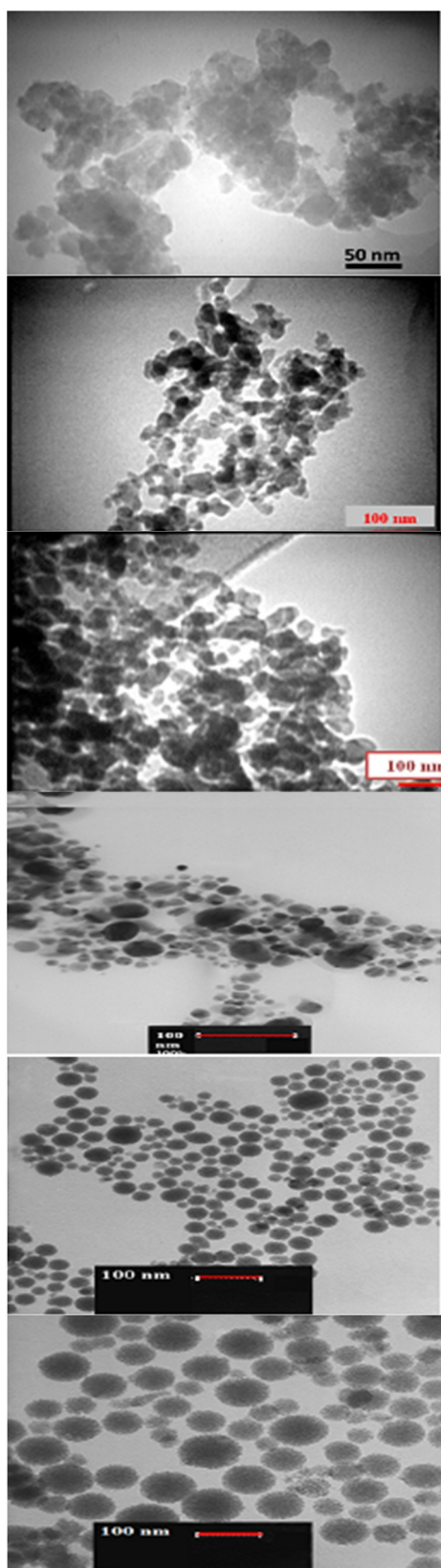
Figure 10. TEM micrograph of TiO_2 nanoparticles at different conditions a: pH=1.8 , b: pH=3.5, c: 36 h stirring time, d: CTAB as a surfactant and e: 550 °C as a temperature, f:650 °C as a temperature

4. CONCLUSION

The sol–gel method was used for the synthesis of nano-TiO_2 from titanium isopropoxide which was coupled with the presence of surface active agents, like CTAB and Span 20. Selection and control of the precise pH, stirring time together with surface active agents proved to be important in controlling the particles size, degree of aggregation and the particles shape. The pH of 3.5 could provide dispersion without agglomeration in nanoparticle powder with rutile and anatase phases; however, at higher pH the powder resulted in the formation of anatase phase. Moreover, the particle size after 36 h, in comparison with 12 ,24 and 48 h, generated a better dispersion as well as finer particles. The microstructural observation showed that nano-TiO_2 powder with CTAB surfactant with 36 h stirring time was produced in the range of 16-20 nm and the implementation of CTAB as a surfactant effectively modified the shape and size distribution of TiO_2 in the structure better than the Span 20 as a surfactant. At last, with increasing the temperature from 450 to 650 °C, the particle sizes of TiO_2 was increased to 30 -33nm, basically spherical shape with good dispersion and without any agglomeration.

5. ACKNOWLEDGMENTS

REFERENCES

1. Saja, S., Taweel, A. and Haider, R., "New route for synthesis of pure anatase TiO_2 nanoparticles via utrasound-assisted sol-gel method", *Journal of Chemical and Pharmaceutical Research*, Vol. 8, No. 2, (2016), 620-626.

2. Zielinska, B. and Borowiak-palen, E., "A study on the synthesis, characterization and photocatalytic activity of TiO_2 derived nanostructures", *Materials Science-Poland*, Vol. 3, (2010),626-639.

3. Choia, H., Stathatos, E. and Dionysios, D., "Sol–gel preparation of mesoporous photocatalytic TiO_2 films and TiO_2/Al_2O_3 composite membranes for environmental applications", *Applied Catalysis B: Environmental*, Vol. 63, (2006), 60-67.

4. Venkatachalam, N., Palanichamy, M. and Murugesan.,V, "Sol–gel preparation and characterization of alkaline earth metal doped nano TiO_2: Efficient photocatalytic degradation of 4chlorophenol", *Journal of Molecular Catalysis A: Chemical*, Vol. 273, (2007), 177-185.

5. Kamil. F., Hubiter, K., Abed, T.K. and Amiery, A.A., "Synthesis of Aluminum and Titanium Oxides Nanoparticles via Sol-Gel Method: Optimization for the Minimum Size", *Journal of nanoscience and technology*, Vol. 2, No. 1, (2016), 37-39.

6. Divya, C., Janarthanan, B., Premkumar, S. and Chandrasekaran, J., "Titanium dioxide nanoparticles preparation for dye sensitized solar cells applications using sol-gel method", *Journal of advanced physical sciences*, Vol. 1, No. 1, (2017), 4-6.

7. Peruma, S., Gnana, C., Monikanda, K. and Ananthakumar, S., "Synthesis and characterization studies of nano TiO$_2$ prepared via sol-gel method", *International Journal of Research in Engineering and Technology,* Vol. 3, (2014), 651-658.

8. Behpour, M. and Chakeri, M., "Ag-doped TiO$_2$ nanocomposite prepared by sol gel method: Photocatalytic Bactericidal Under Visible Light and Characterization", Vol. 2, (2012), 227-234.

9. Manh, N., Thanh, N. and Hoang, N., "Low-temperature synthesis of nano-TiO$_2$ anatase on nafion membrane for using on DMFC", *Journal of Physics: Conference Series*, Vol. 187, (2009), 1-6.

10. Jimmy, C., Jiaguo, Y., Wingkei, Y. and Zhang, L., "Preparation of highly photocatalytic active nano-sized TiO$_2$ particles via ultrasonic irradiation", *Chemical Communications,* (2001), 1942-1943.

11. Macwan, D.P., Pragnesh, N. and Dave, N., "A review on nano-TiO$_2$ sol–gel type syntheses and its applications", *Journal of Materials Science,* Vol.46, (2011), 3669-3686.

12. Miao, Z., Xu, D., Ouyang, J., Guo, G., Zhao, X. and Tang, Y., "Electrochemically induced sol−gel preparation of single-crystalline TiO$_2$ nanowires", *Nano Letters,* Vol. 7, (2002), 716-720.

13. Choi, H., Stathatos, E. and Dionysios, D., "Sol–gel preparation of mesoporous photocatalytic TiO$_2$ films and TiO$_2$/Al$_2$O$_3$ composite membranes for environmental applications", *Applied Catalysis B: Environmental* ,Vol. 63, (2006), 60-67.

14. Zaleska, A., "Doped-TiO$_2$: A review", *Recent patents on Engineering* ,Vol. 2, (2008), 157-164.

15. Harold, P. and Alexander, E.K., "Xray diffraction procedures for polycrystalline and amorphous materials", Willy, New York, (1974).

16. Vetrivel, D., Rajendran, K. and Kalaiselv, V., "Synthesis and characterization of pure titanium dioxide nanoparticles by sol-gel method", *International Journal of Chem Tech Research,* Vol. 7, (2015), 1090-1097.

17. Yang, J., Mei, S. and Ferreira, J., "Surface and sorption properties of TiO$_2$ nanotubes, synthesized by electrochemical anodization", *Materials Science and Engineering: C, Vo*l. 15, (2001), 183-190.

18. Novakovic, R. and Korthaus, B., "Advanced Ceramics for Use in Highly Oxidizing and Corrosive Environment", Trans Tech Publications Ltd, Switzerland, (2001).

19. Billik, P. and Plesch, G., "Mechanochemical synthesis of nanocrystalline TiO$_2$ from liquid TiCl$_4$", *Scripta material*, Vol. 56, (2007), 979-982.

20. Li, J.G., Kamiyama, H., Wang, X.H., Moriyoshi, Y. and Ishigaki, T., "Controlled one-step synthesis of nanocrystalline anatase and rutile TiO$_2$ powders by in-flight thermal plasma oxidation", *Journal of the European Ceramic Society,* Vol. 26, (2004), 15536-15542.

21. Seok, S.I. and Kim, J.H., "Synthesis of TiO$_2$ nanoparticles in porous silica microspheres", *Materials chemistry and physics,* Vol. 86, (2009), 176-182.

22. Prasad, K., Pinjari, D., Pandit, A. and Mhaske, S., "A novel approach to synthesis and characterization of titanium dioxide", *Ultrasonics sonochemistry*, Vol. 17, (2010), 409-415.

23. Abbas, F., Bensaha, R. and Taroré, H., "Regulation of the physical characteristics of titania nanotube", *Comptes Rendus Chimie,* Vol. 17, (2014), 288-275.

24. Fallah, M., Zamani-Meymian, M.-R., Rahimi, R., Rabbani, M., "In vitro bioactivity and corrosion resistance of Zr incorporated TiO$_2$ nanotube arrays for orthopaedic applications", *Applied Surface Science,* Vol. 316, (2016), 264-275.

25. Agartan, L., Kapusuz, D., Park, J. and Ozturk, A., "Effect of initial water content and calcination temperature on photocatalytic properties of TiO$_2$ nanopowders synthesized by the sol–gel process", *Ceramics International,* Vol. 41, (2015), 12788-12797.

26. Leyva-Porras, C., Toxqui-Teran, A., Vega-Becerra, O., Miki-Yoshida, M., Rojas-Villalobos, M., García-Guaderrama, M. and Aguilar-Martínez, J., "Characterization of nanophase titania particles synthesized using in situ steric stabilization", *Journal of Alloys and Compounds,* Vol. 647, (2015), 1755-1765.

27. Yousefi, A., Allahverdi, A. and Hejazi, P., "Effective dispersion of nano-TiO$_2$ powder for enhancement of photocatalytic properties in cement mixes", *Construction and Building Materials,* Vol. 41, (2016), 224-230.

28. Karkare, M., "Choice of precursor not affecting the size of anatase TiO$_2$ nanoparticles but affecting morphology under broader view", *International Nano Letters,* Vol. 4, (2014), 1-9.

29. Lope,. T., Gomez, R., Sanchez, E., Tzompantzi, F. and Vera, L "The effect of calcination temperature on the crystallinity of TiO$_2$", *Journal of Sol-Gel Science and Technology*, Vol. 22, (2003), 363-370.

30. Milani, H. and Nasirian, S., "Decreasing of the activation energy of TiO$_2$ nanoparticles by applying ultrasound waves using the sol-gel method", *Iranian Journal of Physics Research*, Vol. 11, (2012), 411-416.

31. Antoine, R., Dalod, M., Henriksen, L., Grande, T. and Einarsrud, M., "Functionalized TiO$_2$ nanoparticles by single-step", *Journal of Nanotechnology,* Vol. 8, (2017), 304-312.

32. Poursani, A., Nilchi, A., Shariat, S. and Nouri, J., "The Synthesis of Nano TiO$_2$ and Its Use for Removal of Lead Ions from Aqueous Solution", *Journal of Water Resource and Protection,* Vol. 8 ,(2016), 438-448.

33. Rostami, A. and Nasiri, S.M., "Synthesis of mesoporous nanoparticles of TiO$_2$ from ilmenite", *Materials Research Express,* Vol. 4, (2017), 22-30.

34. Zielinsk, B., Borowlak, E., Kalenczuk, R.J., "A study on the synthesis, characterization and photocatalytic activity of TiO$_2$ derived nanostructures", *Materials Science-Poland,* Vol. 28, (2010), 585-594.

35. Gigliola, L., Corrado, B., Federica, G., Giulia, P., "Synthesis and characterization of TiO$_2$ nanoparticles for the reduction of water Pollutants", *Materials*, Vol. 10, (2017), 1208-1219.

36. Qianqian, Y., Jingyu, X., Xiangdong, W., Xiaoling, G. and Tong, Z., "Preparation of highly crystalline mesoporous TiO2 by sol–gel method combined with two-step calcining process", *Journal of Experimental Nanoscience*, Vol. 11, No. 14, (2016), 1127-1137.

37. Divya1, C., Janarthanan, B., Premkumar, B., Chandrasekaran, J., "Titanium dioxide nanoparticles preparation for dye sensitized solar cells applications using sol-gel method", *Journal of Advanced Physical Sciences*, Vol. 1, No. 1, (2017) 4–6.

38. Mane, C., Pawar, R., Gaikwadc, D.,Khobare, R., "Synthesis of TiO$_2$ nanoparticles by Microwave Assisted Sol- Gel Method", *Journal of Medicinal Chemistry and Drug Discovery*, Vol. 2, (2017), 580-584.

39. Doaa, M., Ammar, A., Hanan, A., Hoda, R. and Walied, A., "Preparation and Characterization of Nano Titanium Dioxide Photocatalysts Via Sol Gel Method over Narrow Ranges of Varying Parameters", *Oriental journal of chemistry*, Vol. 33, (2017), 41-51.